Two-Dimensional Angle Estimation for Massive Multiple-Input and Multiple-Output System Based on Hybrid Domain Coding

Rui-Jin Ma[1,2], Hui-Sheng Zhang[1]

[1] Institute of Electronic and Information, Northwestern Polytechnical University, China
[2] China Mobile Communications Group Shaanxi Co., Ltd.
13891881066@139.com, zhanghuisheng@nwpu.edu.cn

Abstract

This paper aims to reduce the complexity of angle estimation in massive multiple-input and multiple-output (MIMO) systems. For this purpose, the hybrid domain coding was adopted to reduce the dimension of the received signal, and thus the computing load to find the inverse matrix. To improve the vector estimation accuracy of sub-array signal space, a new estimation method of signal parameters via rotational invariant techniques (ESPRIT) was proposed based on hybrid domain coding and the least squares (LS) method. The direction of arrival equation is also derived. Finally, the root-mean-square error (RMSE) and runtime of the proposed method were compared with those of some other methods through simulation. The results verify the effectiveness and reliability of the algorithm. The research findings lay the basis for accurate channel estimation of massive MIMO systems.

Keywords: Multiple-input and multiple-output (MIMO), ESPRIT, Root-mean-square error (RMSE)

1 Introduction

The 5th-generation wireless systems (5G) outperform 4G in transmission rate and spectrum efficiency. The key to implementing 5G lies in the massive multiple-input and multiple-output (MIMO) system. Since its birth, the massive MIMO has attracted much attention from scholars at home and abroad. By this technology, more antennas are provided at the base station and the client to enhance the system performance [1-3]. For massive MIMO, the accuracy of channel estimation directly hinges on the direction of arrival (DOA) in the angle domain. Therefore, the DOA has become a hotspot in the research of massive MIMO channel estimation [4-5]. The DOA involves two dimensions, namely, the angle of departure (AOD) and the angle of arrival (AOA).

As a fundamental issue in array processing, angle estimation has been acknowledged as an important task in radar, sonar and communications. Many algorithms rely on array antennas to estimate the angle, including maximum likelihood estimation, entropy spectrum estimation and eigen-decomposition. Among them, the multiple signal classification (MUSIC) algorithm is a typical subspace algorithm based on eigen-decomposition [6-7]. The core idea is to estimate the angle through space division based on the orthogonality of the signal subspace and the noise subspace. Since the parameters are estimated by searching for spectral peaks, the MUSIC algorithm may incur a heavy computing load to fulfill a high operating accuracy. To solve the problem, the root-MUSIC algorithm has been developed [8]. Another popular algorithm is the estimation of signal parameters via rotational invariant techniques (ESPRIT) [9]. Based on subspace rotation invariant technology, the ESPRIT features a low computing load because it does not need to search for spatial spectrum. The advantage of the ESPRIT algorithm is that it can decrease the computation time and improve the feasibility. However, the disadvantage of ESPRIT algorithm is that it can't process the coherent sources. On this basis, the 2D ESPRIT algorithm has been created to realize 2D angle estimation [10-11]. This algorithm is adopted for our research to improve the angle estimation performance. Compared to MUSIC algorithm, the ESPRIT has an advantage in estimating the practical AoA and AoD with continuous than discrete values.

Angle estimation plays an important role in channel estimation in the angle domain. In a massive MIMO system, the transmitting end transmits the pilot beams, while the receiving end processes the best-performing beam among all the received beams. When there are many antennas at the transmitting end, the training load of the system increases linearly with the growth in the number of antennas. Therefore, the received beams must be compressed by signal processing in the massive system. A viable option for the compression is the hybrid domain coding strategy. By this method, a hybrid analog-to-digital converter is installed at the transmitting and receiving ends, offering a comprehensive

*Corresponding Author: Rui-Jin Ma; 13891881066@139.com
DOI: 10.3966/160792642018091905025

plan for beam quantity, system power and implementation complexity. Much research has been done on the analog-digital hybrid structure at both ends. For instance, Reference [12] designs a low-complexity encoder through hybrid domain coding at the transmitting end. Reference [13] proposes a plan for arranging more transmitting antennas, aiming to compensate for the declining sum rate of hybrid domain coding with the growth in the dimension of all-digital beamforming. Reference [14] presents a recursive hybrid domain beam performance algorithm under single-user millimeter wave conditions, which can achieve faster rate without limiting the digital beamforming method. In this paper, hybrid domain coding is applied to both transmitting and receiving ends, and the least squares (LS) method was combined with 2D ESPRIT for hybrid domain coding into a LS hybrid domain ESPRIT (HYLS-ESPRIT). Then, the HYLS-ESPRIT was applied to estimate the AOD and AOA of the massive MIMO system. The results show that the proposed method can improve the accuracy of angle estimation without reducing the computing load of the system. The research findings lay a solid basis for accurate channel estimation.

The remainder of this paper is organized as follows: Section 2 introduces the system model of hybrid domain massive MIMO; Section 3 reviews the ESPRIT based on hybrid domain coding, puts forward the HYLS-ESPRIT, and applies the proposed method to estimate the AOD and the AOA; Section 4 compares the estimation results of the proposed method and those of traditional methods through simulation; Section 5 wraps up this paper with some meaningful conclusions.

Notations: The italic bold face lower and upper symbols describe the column vectors and matrices respectively. $(\cdot)^{-1}$, $(\cdot)^{H}$, $\|\cdot\|_2$ denote the inversion, conjugate transpose and l_2 norm.

2 Hybrid Domain Massive MIMO System Model

We consider a typical massive MIMO system transmission model with hybrid coding, as shown in Figure 1.

As shown in Figure 1, N_t and N_r are the number of antennas at the transmitting ends and receiving ends, respectively, N_t^{RF} and N_r^{RF} are the number of radio frequency (RF) chains at the transmitting and receiving ends, respectively. Note that $N_t^{RF} \le N_t$ and $N_r^{RF} \le N_r$. The RF chain beamforming was simulated by an analog phase shifter. To reduce the system power consumption, the multiple transmitting antennas of the massive MIMO system were replaced by a few RF chains. As shown in Figure 1, the transmitting end model can be described as:

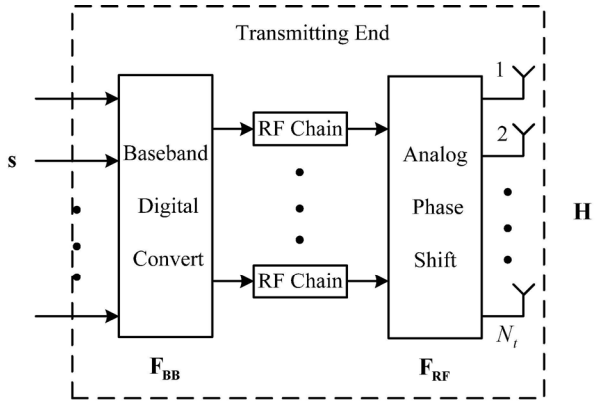

(a) Transmitting End

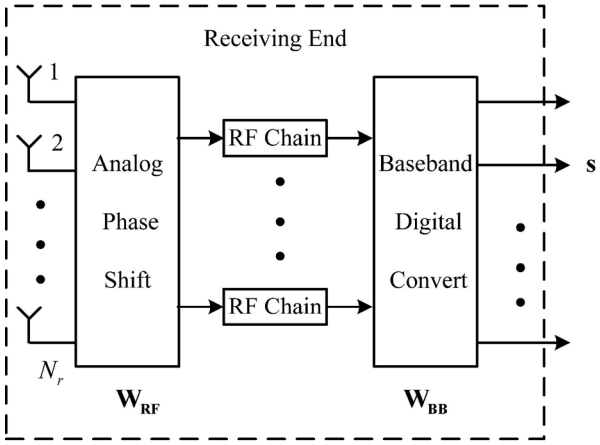

(b) Receiving End

Figure 1. Hybrid domain massive MIMO model

$$\mathbf{X} = \mathbf{F}\mathbf{s} + \mathbf{N}, \tag{1}$$

where $\mathbf{F} \in \mathbb{C}^{2N_t \times N_t^{RF}}$ is the hybrid domain coding matrix of the transmitting end; $\mathbf{s}$ is the transmitted signal; $\mathbf{N}$ is the Gaussian white noise signal. $\mathbf{F}$=$\mathbf{F}_{RF}\mathbf{F}_{BB}$ with $\mathbf{F}_{RF}$ and $\mathbf{F}_{BB}$ being the analog phase conversion matrix and baseband digital conversion matrix at the transmitting end, respectively. The hybrid domain coding architecture at the receiving end is similar to that at the transmitting end. Thus, the receiving end model can be described as:

$$\begin{aligned} \mathbf{Y} &= \mathbf{W}^{\mathbf{H}}\mathbf{H}\mathbf{F}\mathbf{R}_{\mathbf{ss}} + \mathbf{W}^{\mathbf{H}}\mathbf{N} \\ &= \sqrt{\mathbf{P}}\mathbf{W}^{\mathbf{H}}\mathbf{H}\mathbf{F} + \bar{\mathbf{N}} \end{aligned}, \tag{2}$$

where $\mathbf{W} \in \mathbb{C}^{2N_r \times N_r^{RF}}$ is the hybrid domain coding matrix of the receiving end. $\bar{\mathbf{N}}$ is also the Gaussian white noise signal. $\mathbf{W}$=$\mathbf{W}_{RF}\mathbf{W}_{BB}$ with $\mathbf{W}_{RF}$ and $\mathbf{W}_{RF}$ being the analog phase conversion matrix and baseband digital conversion matrix at the receiving end, respectively. From the above equation, it can be seen that the dimension of the received signal is smaller than that without using hybrid domain coding. Thus,

the use of hybrid domain coding can effectively reduce the amount of data to be processed.

3 ESPRIT Algorithm Based on Hybrid Domain Coding

3.1 ESPRIT Algorithm for AOD and AOA Estimation

Suppose there is an array with N_t pairs of transmitting elements, each of which has two elements with the same response features. Let Δ be the phase shift between the two elements. It is assumed that some far-field narrow-band signals, which are independent of each other, are incident on the array in the form of plane waves, the signal sources have the same center frequency f_0, and thearrival of signals is a zero-meanrandom process.

Divide the array $\mathbf{Z}_x$ at the transmitting end into sub-arrays $\mathbf{Z}_{x1}$ and $\mathbf{Z}_{x2}$:

$$\mathbf{Z}_x=\begin{bmatrix}\mathbf{Z}_{x1}\\ \mathbf{Z}_{x2}\end{bmatrix}=\begin{bmatrix}x_1^1,x_1^2,\cdots,x_1^{N_t}\\ x_2^1,x_2^2,\cdots,x_2^{N_t}\end{bmatrix}, \tag{3}$$

Then, $x_{1i}(t)$ and $x_{2i}(t)$ are the output signals of the two sub-arrays for the i-th element pair, which can be expressed as:

$$x_{1i}(t)=\sum_{p=1}^{P}s_p(t)a_i(\boldsymbol{\theta}_p)+n_{x1}(t), \tag{4.a}$$

$$x_{2i}(t)=\sum_{p=1}^{P}s_p(t)e^{\frac{j2\pi f_0\Delta\sin\boldsymbol{\theta}_p}{C}}a_i(\boldsymbol{\theta}_p)+n_{x2}(t), \tag{4.b}$$

where $s_p(t)$ is the p-th signal transmitted by the reference array element; $\boldsymbol{\theta}_p$ is the AOD of the wave from the p-th target source; $a_i(\theta_p)$ is the response of the i-th element pair to the p-th signal source; C is the speed of light; $n_{x1}(t)$ and $n_{x2}(t)$ are the additive Gaussian white noises on the i-th element pair. Thus, the vector expressions of the above equations are as follows:

$$\mathbf{x}_1(t)=\mathbf{A}\mathbf{s}(t)+\mathbf{n}_{x1}(t), \tag{5.a}$$

$$\mathbf{x}_2(t)=\mathbf{A}\boldsymbol{\Phi}\mathbf{s}(t)+\mathbf{n}_{x2}(t), \tag{5.b}$$

where $\mathbf{A}\in\mathbb{C}^{N_t\times P}$ and:

$$\mathbf{A}=\begin{bmatrix}a_1(\boldsymbol{\theta}_1) & a_1(\boldsymbol{\theta}_2) & \cdots & a_1(\boldsymbol{\theta}_P)\\ a_2(\boldsymbol{\theta}_1) & a_2(\boldsymbol{\theta}_2) & \cdots & a_2(\boldsymbol{\theta}_P)\\ \vdots & \vdots & \ddots & \vdots\\ a_{N_t}(\boldsymbol{\theta}_1) & a_{N_t}(\boldsymbol{\theta}_2) & \cdots & a_{N_t}(\boldsymbol{\theta}_P)\end{bmatrix}, \tag{6}$$

where the rotation factor $\boldsymbol{\Phi}\in\mathbb{C}^{P\times P}$. where the transmitted signal is:

$$\mathbf{s}(t)=[s_1(t),s_2(t),\cdots,s_P(t)]^T, \tag{7}$$

Owing to the shift-invariance of the sub-arrays, the signals of the sub-arrays are also shift-invariant. Hence, the signal of sub-array $\mathbf{Z}_{x2}$ equals the product between that of sub-array $\mathbf{Z}_{x1}$ and the rotation factor $\boldsymbol{\Phi}$, and:

$$\boldsymbol{\Phi}=\begin{bmatrix}e^{\frac{j2\pi f_0\Delta\sin\boldsymbol{\theta}_1}{C}} & 0 & \cdots & 0\\ 0 & e^{\frac{j2\pi f_0\Delta\sin\boldsymbol{\theta}_2}{C}} & \cdots & 0\\ \vdots & \vdots & \ddots & \vdots\\ 0 & 0 & \cdots & e^{\frac{j2\pi f_0\Delta\sin\boldsymbol{\theta}_P}{C}}\end{bmatrix}, \tag{8}$$

From the above equation, we can see that the diagonal elements of the matrix $\boldsymbol{\Phi}$ contain the direction of the AOD $\boldsymbol{\Phi}$. Equation (8) and Equation (5) can be combined as:

$$\mathbf{x}=\begin{bmatrix}\mathbf{x}_1(t)\\ \mathbf{x}_2(t)\end{bmatrix}=\bar{\mathbf{A}}\mathbf{s}(t)+\mathbf{n}_x(t), \tag{9}$$

where The matrix form of Equation (9) can be expressed as:

$$\mathbf{X}=\bar{\mathbf{A}}\mathbf{S}+\mathbf{N}_x, \tag{10}$$

Divide the array at the receiving end into sub-arrays $\mathbf{Z}_{y1}$ and $\mathbf{Z}_{y1}$:

$$\mathbf{Z}_y=\begin{bmatrix}\mathbf{Z}_{y1}\\ \mathbf{Z}_{y2}\end{bmatrix}=\begin{bmatrix}y_1^1,y_1^2,\cdots,y_1^{N_t}\\ y_2^1,y_2^2,\cdots,y_2^{N_t}\end{bmatrix}, \tag{11}$$

According to the model of the transmitting end, the data matrix of the array at the receiving end can be expressed as:

$$\mathbf{Y}=\bar{\mathbf{B}}\mathbf{S}+\mathbf{N}_y, \tag{12}$$

where

$$\mathbf{B}=\begin{bmatrix}b_1(\varphi_1) & b_1(\varphi_2) & \cdots & b_1(\varphi_P)\\ b_2(\varphi_1) & b_2(\varphi_2) & \cdots & b_2(\varphi_P)\\ \vdots & \vdots & \ddots & \vdots\\ b_{N_r}(\varphi_1) & b_{N_r}(\varphi_2) & \cdots & b_{N_r}(\varphi_P)\end{bmatrix}, \tag{13}$$

$$\boldsymbol{\Omega}=\begin{bmatrix}e^{\frac{j2\pi f_0\Delta\sin\varphi_1}{C}} & 0 & \cdots & 0\\ 0 & e^{\frac{j2\pi f_0\Delta\sin\varphi_2}{C}} & \cdots & 0\\ \vdots & \vdots & \ddots & \vdots\\ 0 & 0 & \cdots & e^{\frac{j2\pi f_0\Delta\sin\varphi_P}{C}}\end{bmatrix}, \tag{14}$$

where φ_p is the AOA of the wave from the *p*-th target source; $\overline{\mathbf{B}}=\begin{bmatrix}\mathbf{B}\\ \mathbf{B\Omega}\end{bmatrix}$. Combining the matrix of the arrays at the transmitting and receiving ends, we have the cross-correlation matrix of the signal matrices ***X*** and ***Y***:

$$\mathbf{R}_{XY}=E\left[\mathbf{X}\mathbf{Y}^H\right]=\sqrt{P}\overline{\mathbf{A}}\mathbf{R}_{ss}\overline{\mathbf{B}}^H+\sigma^2\mathbf{I}, \quad (15)$$

Where $\mathbf{R}_{ss}$ is the correlation matrix of $\mathbf{S}$.

3.2 Angle Estimation Based on HYLS-ESPRIT

In this section, we propose a 2D HYLS-ESPRIT bseed super-resolution channel estimation scheme for missive MIMO system with hybrid domain coding. According to the model of hybrid domain massive MIMO system, the function of Equation (15) is similar to that of ***H*** in Equation (2).

Substituting Equation (15) into Equation (2), the received data $\mathbf{Y}$ can be shown:

$$\begin{aligned}\mathbf{Y}&=P\mathbf{W}^H\overline{\mathbf{A}}\mathbf{R}_{ss}\overline{\mathbf{B}}^H\mathbf{F}+\mathbf{N}_y\\ &=P\mathbf{W}^H\begin{bmatrix}\mathbf{A}\\ \mathbf{A\Phi}\end{bmatrix}\mathbf{R}_{ss}\left[\mathbf{B}\ \ \mathbf{B\Omega}\right]\mathbf{F}+\mathbf{N}_y\end{aligned}, \quad (16)$$

where $\mathbf{N}_y$ denotes the noise matrix.

The AOD $\boldsymbol{\theta}$ can be solved in the following steps:

Perform eigen-decomposition of $\mathbf{Y}$:

$$\mathbf{Y}=\sum_{n_t=1}^{2N_t}\lambda_x^{n_t}\mathbf{e}_x^{n_t}(\mathbf{e}_x^{n_t})^H=\mathbf{E}_{sx}\mathbf{\Lambda}_{sx}\mathbf{E}_{sx}^H+\sigma^2\mathbf{E}_{nx}\mathbf{E}_{nx}^H, \quad (17)$$

where eigenvalue $\mathbf{E}_{sx}$ is the signal subspace formed by eigenvectors $\left[\mathbf{e}_x^1,\mathbf{e}_x^2\cdots\mathbf{e}_x^P\right]$; $\mathbf{E}_{nx}$ is the noise subspace formed by eigenvectors $\left[\mathbf{e}_x^{P+1},\mathbf{e}_x^{P+2}\cdots\mathbf{e}_x^{2N_t}\right]$ which is orthogonal to the signal subspaces. Hence, there is a full rank matrix $\mathbf{T}_x$ such that:

$$\mathbf{E}_{sx}=\mathbf{W}^H\overline{\mathbf{A}}\mathbf{T}_x=\begin{bmatrix}\mathbf{W}^H\mathbf{A}\mathbf{T}_x\\ \mathbf{W}^H\mathbf{A\Phi}\mathbf{T}_x\end{bmatrix}=\begin{bmatrix}\mathbf{E}_{sx1}\\ \mathbf{E}_{sx2}\end{bmatrix}, \quad (18)$$

From the above equation, we have:

$$\mathbf{E}_{sx2}=\mathbf{E}_{sx1}\mathbf{T}_x^{-1}\mathbf{\Phi}\mathbf{T}_x, \quad (19)$$

Under the LS criterion, $\mathbf{E}_{sx1}$ and $\mathbf{E}_{sx2}$ expand to the same subspace. Thus, there is a full rank matrix $\mathbf{Q}_x$, that is:

$$\mathbf{Q}_x=\begin{bmatrix}\mathbf{Q}_{x1}\\ \mathbf{Q}_{x2}\end{bmatrix} \text{ is orthogonal to } \left[\mathbf{E}_{sx1}\ \ \mathbf{E}_{sx2}\right].$$

Thus, we have:

$$\mathbf{E}_{sx}\mathbf{Q}=0, \quad (20)$$

The above equation can be expanded as:

$$\begin{aligned}&\left[\mathbf{E}_{sx1}\ \ \mathbf{E}_{sx2}\right]\begin{bmatrix}\mathbf{Q}_{x1}\\ \mathbf{Q}_{x2}\end{bmatrix}\\ &=\mathbf{E}_{sx1}\mathbf{Q}_{x1}+\mathbf{E}_{sx2}\mathbf{Q}_{x2}\\ &=\mathbf{W}^H\mathbf{A}\mathbf{T}_x\mathbf{Q}_{x1}+\mathbf{W}^H\mathbf{A\Phi}\mathbf{T}\mathbf{Q}_{x2}\\ &=0\end{aligned}, \quad (21)$$

The above equation can be simplified as:

$$-\mathbf{W}^H\mathbf{A}\mathbf{T}_x\mathbf{Q}_{x1}\mathbf{Q}_{x2}^{-1}=\mathbf{W}^H\mathbf{A\Phi}\mathbf{T}_x, \quad (22)$$

Thus:

$$-\mathbf{E}_{sx1}\mathbf{Q}_{x1}\mathbf{Q}_{x2}^{-1}=\mathbf{E}_{sx2}, \quad (23)$$

Suppose:

$$\mathbf{Q}_x=-\mathbf{Q}_{x1}\mathbf{Q}_{x2}^{-1}, \quad (24)$$

The above two equations can be combined as:

$$\mathbf{E}_{sx1}\mathbf{Q}_x=\mathbf{E}_{sx2} \quad (25)$$

Thus:

$$\mathbf{Q}_x=\mathbf{E}_{sx1}^{-1}\mathbf{E}_{sx2}, \quad (26)$$

$$\mathbf{W}^H\mathbf{A}\mathbf{T}\mathbf{Q}_x=\mathbf{W}^H\mathbf{A\Phi}\mathbf{T}, \quad (27)$$

$$\mathbf{\Phi}=\mathbf{T}_x\mathbf{Q}_x\mathbf{T}_x^{-1}, \quad (28)$$

Therefore, $\mathbf{\Phi}$ and $\mathbf{Q}_x$ have the same eigenvalue, which is the diagonal element of $\mathbf{\Phi}$. The eigenvalue $\lambda_x^p(p=1,2,\cdots,P)$ can be solved according to $\mathbf{Q}_x$

Thus, the AOD can be estimated as:

$$\hat{\theta}_p=\arcsin\left(\frac{C\cdot angle(\lambda_x^p)}{2\pi f_0\Delta}\right), \quad (29)$$

The AOA φ can be solved in the following steps:

Perform eigen-decomposition of $\mathbf{Y}^H$, the transpose transposition matrix of $\mathbf{Y}$:

$$\begin{aligned}\mathbf{Y}^H&=P\mathbf{W}^H\overline{\mathbf{A}}\mathbf{R}_{ss}\overline{\mathbf{B}}^H\mathbf{F}+\mathbf{N}_y\\ &=P\mathbf{F}^H\begin{bmatrix}\mathbf{B}\\ \mathbf{B\Omega}\end{bmatrix}\mathbf{R}_{ss}\left[\mathbf{A}\ \ \mathbf{A\Phi}\right]\mathbf{W}+\mathbf{N}_y\end{aligned}, \quad (30)$$

Perform eigen-decomposition:

$$\mathbf{Y}^H=\sum_{n_r=1}^{2N_r}\lambda_y^{n_r}\mathbf{e}_y^{n_r}(\mathbf{e}_y^{n_r})^H=\mathbf{E}_{sy}\mathbf{\Lambda}_{sy}\mathbf{E}_{sy}^H+\sigma^2\mathbf{E}_{ny}\mathbf{E}_{ny}^H, \quad (31)$$

Similar to the estimation of the AOD, we define the following parameters:

$\mathbf{E}_{sy}$ is the signal subspace formed by eigenvectors $\left[\mathbf{e}_y^1,\mathbf{e}_y^2\cdots\mathbf{e}_y^P\right]$; $\mathbf{E}_{ny}$ is the noise subspace formed by eigenvectors $\left[\mathbf{e}_y^{P+1},\mathbf{e}_y^{P+2}\cdots\mathbf{e}_y^{2N_t}\right]$ which is orthogonal to

the signal subspaces. Through the analysis on the AOA, we have a matrix $\mathbf{Q}_y$ similar to $\mathbf{\Omega}$:

$$\mathbf{Q}_y = \mathbf{E}_{sy1}^{-1}\mathbf{E}_{sy2}, \tag{32}$$

$$\mathbf{E}_{sy} = \mathbf{F}^H\bar{\mathbf{B}}\mathbf{T}_y = \begin{bmatrix} \mathbf{F}^H\mathbf{B}\mathbf{T}_y \\ \mathbf{F}^H\bar{\mathbf{B}}\mathbf{\Omega}\mathbf{T}_y \end{bmatrix} = \begin{bmatrix} \mathbf{E}_{sy1} \\ \mathbf{E}_{sy2} \end{bmatrix}, \tag{33}$$

where $\mathbf{T}_y$ is also a full rank matrix.

The eigenvalue $\lambda_y^p (p = 1,2,\cdots,P)$ can be solved according to $\mathbf{Q}_y$.

Thus, the AOAcan be estimated as:

$$\varphi_p = \arcsin\left(\frac{C \cdot angle(\lambda_y^p)}{2\pi f_0 \Delta}\right), \tag{34}$$

4 Simulation

Suppose there are three signal sources, whose (AOD, AOA) are (40°, 45°), (50°, 55°) and (60°, 65°) respectively. The arrays are *L*-shaped, linear and uniformly distributed. In each array, the elements are arranged at an interval of half-wavelength. The other parameters are listed in Table 1.

Table 1. Parameter settings

Name	Value
Number of transmitting arrays N_t	16
Number of receiving arrays N_r	16
Hybrid domain transmitting RF chains N_t^{RF}	8
Hybrid domain receiving RF chains N_r^{RF}	8
Number of target sources	3
Number of snapshots	100
Signal-to-noise ratio (dB)	0~30
Number of Monte-Carlo simulations	200
Transmitting frequency (Hz)	4G

As the judgement criteria for accuracy, the root-mean-square error (RMSE) can be defined as [15].

$$RMSE = \sqrt{\frac{1}{Num}\sum_{m=1}^{Num}\left|\gamma_m - \gamma_0\right|^2} \tag{35}$$

where Num is the number of simulations; γ_m is the estimated value γ_0 at the m-thsimulation angle; γ is the AOD or AOA.

Figure 2 simulates the estimated AOD and AOA of the proposed HYLS-ESPRIT algorithm in the massive MIMO system at the signal-to-noise ratio (SNR) of 20dB. A total of 200 Monte-Carlo simulations were carried out. From Figure.2, we can see that the AOA and AOD can be estimated correctly and the feasibility of the HYLS-ESPRIT algorithm is also valid.

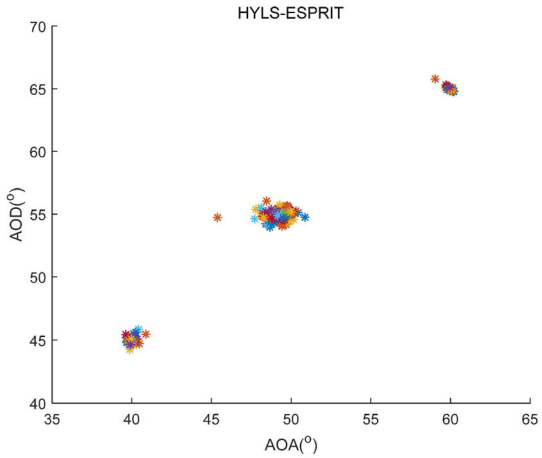

Figure 2. 2D angle estimation results of hybrid domain coding at SNR=20dB

Figures 3 and 4 respectively present the RMSEs of the AOD and AOA estimated by the proposed HYLS-ESPRIT algorithm under different number of signal sources. Comparing the two figures, it is clear that the angle estimation error increased with the number of target sources.

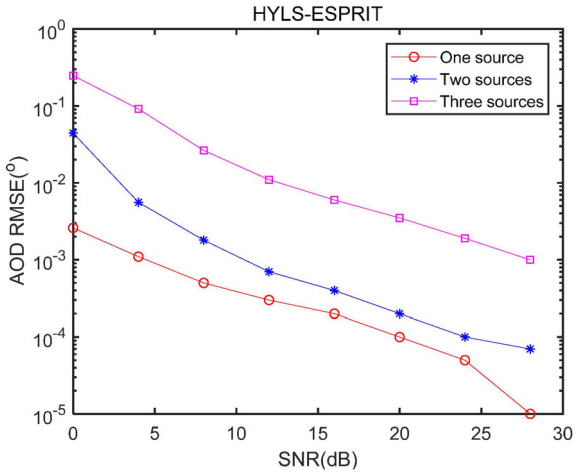

Figure 3. AOD estimated by hybrid domain coding at different number of target sources

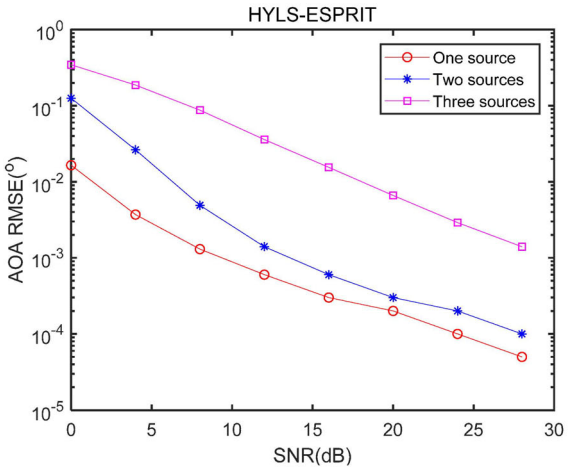

Figure 4. AOA estimated by hybrid domain coding at different number of target sources

It can be observed frm Figure 3 and Figure 4 that the number of the sources plays an important part in the estimation performance. The more the number of the source, the worse the RMSE.

To verify the effectiveness of the proposed algorithm, the proposed HYLS-ESPRIT algorithm was contrasted with the traditional ESPRIT algorithm and the MUSIC algorithm. Figures 5 and Figure 6 compare the RMSE of these different algorithms.

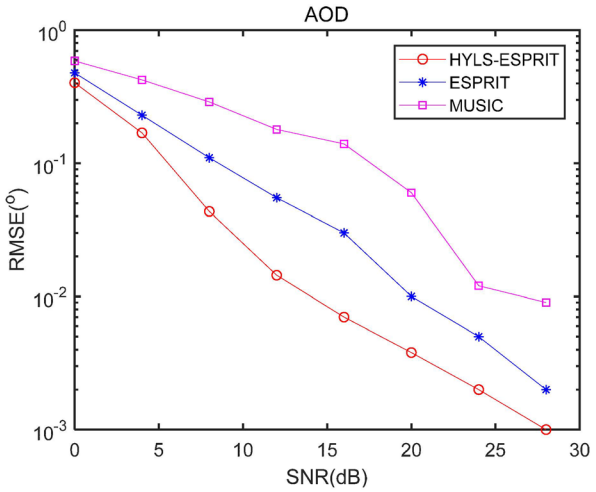

Figure 5. AOD RMSE of different algorithms

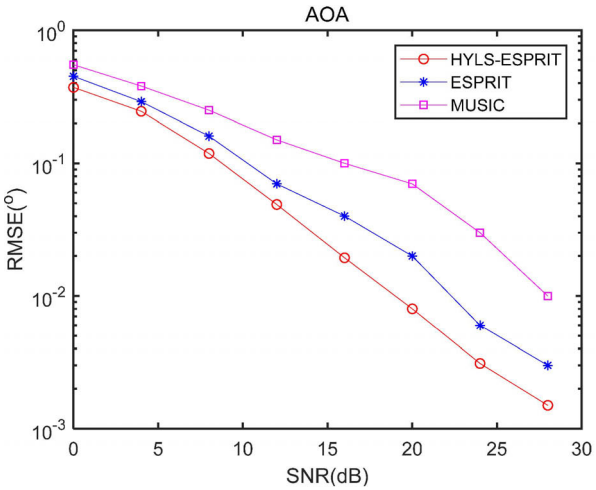

Figure 6. AOA RMSE of different algorithms

The results in Figures 5 and 6 show that the estimated AOD and AOA of the HYLS-ESPRIT were superior than those of the traditional ESPRIT algorithm and MUSIC algorithm. The RMSE performance of HYLS-ESPRIT has an advantage about 3.5db than ESPRIT algorithm, 6db than MUSIC algorithm. From the results, we can also see that the MUSIC algorithm had the worst estimation of the two angles.

Figure 7 describes the computational time of all methods including HYLS-ESPRIT, ESPRIT and MUSIC method. From Figure 7, we can see that the HYLS-ESPRIT algorithm has much lower complexity than the other two methods for the reason that the hybrid domain coding decreases the dimension of the received information (the dimension of ESPRIT and MUSIC are both fixed to 32×32, the dimension of HYLS-ESPRIT is fixed to 8×8) and improves the running time performance. As for the computing speed (Figure 7), the MUSIC was the least efficient algorithm, because it relies on the search for spectral peaks. By contrast, the HYLS-ESPRIT was much faster than the traditional ESPRIT, as the data dimension is effectively reduced by the hybrid domain coding.

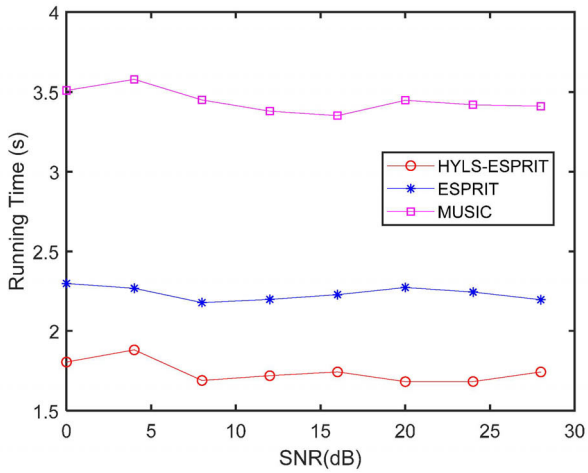

Figure 7. Runtime of different lgorithms

5 Conclusions

This paper applies the ESPRIT to the estimation of 2D DOA of the massive MIMO system. To reduce system complexity, the hybrid domain coding was adopted simultaneously at both transmitting and receiving ends. Then, the ESPRIT algorithm for AOD and AOA estimation was introduced in details. On this basis, the HYLS-ESPRIT was proposed, together with its AOD and AOA equations. The RMSE and runtime of the proposed algorithm were contrasted with some other methods. Through simulation, it is learned that the HYLS-ESPRIT outperforms the traditional ESPRIT and MUSIC algorithms in accuracy and efficiency under the adoption of the hybrid domain coding. The research findings lay the basis for accurate channel estimation of massive MIMO systems.

Further work in this area includes codebook-based method for hybrid channel information feedback in massive MIMO systems, fast channel tracking for beamspace massive MIMO systems and so on.

References

[1] F. Boccardi, R. W. Heath, A. Lozano, T. L. Marzetta, P. Popovski, Five Disruptive Technology Directions for 5G, *IEEE Communications Magazine*, Vol. 52, No. 2, pp. 74-80, February, 2014.

[2] E. L. Bengtsson, F. Rusek, S. Malkowsky, F. Tufvesson, P. C. Karlsson, O. Edfors, A Simulation Framework for Multiple-

Antenna Terminals in 5G Massive MIMO Systems, *IEEE Access*, Vol. 5, pp. 26819-26831, November, 2017.

[3] D. M. Wang, Y. Zhang, H. Wei, X. You, X. Gao, J. Wang, An Overview of Transmission Theory and Techniques of Large-scale Antenna Systems for 5G Wireless Communications, *Scientia Sinica Informationis*, Vol. 46, No. 1, pp. 3-21, January, 2016.

[4] L. Zhao, G. Geraci, T. Yang, D. W. K. Ng, J. Yuan, A Tone-based AoA Estimation and Multiuser Precoding for Millimeter Wave Massive MIMO, *IEEE Transactions on Communications*, Vol. 65, No. 12, pp. 5209-5225, December, 2017.

[5] T. Younas, J. Li, J. Arshad, M. M. Tulu, Performance Analysis of Improved ZF Algorithm for Massive MIMO in Uplink, *Electronics Letters*, Vol. 52, No. 23, pp. 1554-1556, November, 2017.

[6] W. Liao, MUSIC for Multidimensional Spectral Estimation: Stability and Super-Resolution, *IEEE Transactions on Signal Processing*, Vol. 63, No. 23, pp. 6395-6406, December, 2015.

[7] A. C. Fannjiang, The MUSIC Algorithm for Sparse Objects: A Compressed Sensing Analysis, *Inverse Probelems*, Vol. 27, No. 3, pp. 35013, March, 2011.

[8] W. Liao, MUSIC for Joint Frequency Estimation: Stability with Compressive Measurements, *IEEE Global Conference on Signal and Information Processing*, Altanta, GA, 2014, pp. 414-418.

[9] J. Zhang, M. Haardt, Channel Estimation and Training Design for Hybrid Multi-carrier MmWave Massive MIMO Systems: The Beamspace ESPRIT Approach, *2017 5th European Signal Processing Conference*, Kos, Greece, 2017, pp. 385-389.

[10] Y. Zhou, Z. Fei, S. Yang, J. Kuang, S. Chen, L. Hanzo, Joint Angle Estimation and Signal Reconstruction for Coherently Distributed Sources in Massive MIMO Systems Based on 2D Unitary ESPRIT, *IEEE Access*, Vol. 5, pp. 9632-9646, May, 2017.

[11] A. Liao, Z. Gao, Y. Wu, H. Wang, M.-S. Alouini, 2D Unitary ESPRIT Based Super-Resolution Channel Estimation for Millimeter-Wave Massive MIMO with Hybrid Precoding, *IEEE Access*, Vol. 5, pp. 24747-24757, November, 2017.

[12] X. Yu, J.-C. Shen, J. Zhang, K. B. Letaief, Alternating Minimization Algorithms for Hybrid Precoding in Millimeter Wave MIMO Systems, *IEEE Journal of Selected Topics in Signal Processing*, Vol. 10, No. 3, pp. 485-500, April, 2016.

[13] D. Ying, F. W. Vook, T. A. Thomas, D. J. Love, Hybrid Structure in Massive MIMO: Achieving Large Sum Rate with Fewer RF Chains, *IEEE International Conference on Communications*, London, UK, 2015, pp. 2344- 2349.

[14] A. Alkhateeb, O. E. Ayach, G. Leus, R. W. Heath, Hybrid Precoding for Millimeter Wave Cellular Systems with Partial Channel Knowledge, *IEEE Information Theory and Applications Workshop*, San Diego, CA, 2013, pp. 1-5.

[15] X. F. Zhang, F. Wang, D. Z. Xu, *Zhenlie Xinhao Chuli De Lilun He Yingyong*, National Defense Industry Press, 2010.

Biographies

RuiJin Ma is currently a doctoral students at Institute of Electronic and Information, Northwestern Polytechnical University, China. she is also a senior engineer of China Mobile Communications Group Shaanxi Co., Ltd. Her research interests cover Communication systems theory and technology, multimedia communications and networking technologies.

HuiSheng Zhang is currently an professor and Doctoral Tutor at Institute of Electronic and Information, Northwestern Polytechnical University, China. His research interests cover Communication systems theory and technology, satellite communications, multimedia communications and networking technologies, and satellite-based navigation and positioning techniques.